

8 SCIENTIFIC HIGHLIGHT OF THE MONTH: "Relativistic Effects and Disordered Local Moments in Magnets"

Relativistic Effects and Disordered Local Moments in Magnets

Julie B. Staunton

Department of Physics, University of Warwick, Coventry CV4 7AL, U.K.

email:j.b.staunton@warwick.ac.uk

Abstract

A brief review of the 'disordered local moment' (DLM) theory of magnetism at finite temperatures is given. This has recently been enhanced so that it includes relativistic (R) effects such as spin-orbit coupling. The relevance of the R-DLM theory for providing an ab-initio account of the temperature dependence of magnetic properties including magnetotransport is stressed. Magnetic anisotropy is discussed in particular. In this context a new magnetic torque based method is described and demonstrated with an application to iron nanoclusters on a platinum substrate. The R-DLM theory is illustrated by a study of the temperature dependence of the magnetic anisotropy of the technologically important *FePt* alloy in both its magnetically hard $L1_0$ -ordered and soft cubic compositionally disordered phases.

Acknowledgements: It is a pleasure to acknowledge the collaboration of many colleagues on the various aspects occurring in this selective review: in particular *S.Bornemann*, *J.Minar* and *H.Ebert* on the magnetic torque calculations on deposited clusters (see [1]) and *B.Gyorffy*, *S.Ostapin*, *S.S.A.Razee*, *L.Szunyogh*, *A.Buruzs*, *L.Udvardi* and *P.Weinberger* on the development of the R-DLM theory (see [2-4]).

1 Introduction

In principle, relativistic density functional theory [5] (R-DFT) can describe a magnetic material completely, providing a free energy, F , ab initio. F is a functional of the magnetisation, $\mathbf{M}(\mathbf{r})$. For a ferromagnetic material the magnetisation is often characterised in terms of M_s , the saturation magnetisation and a direction $\mathbf{n} = (n_x, n_y, n_z)$ which is assumed to vary over length scales long compared with atomic ones, i.e. $\mathbf{M}(\mathbf{r}) = M_s \mathbf{n}(\mathbf{r})$. F can now be approximated by the familiar micromagnetic sum of an exchange term with exchange constant A , an anisotropy term involving K , a magnetocrystalline anisotropy constant, a term describing the interaction with an applied magnetic field and finally a magnetostatic 'shape anisotropy' term [6]. Materials are typically characterised by a set of M_s , A and K constants combined into two important length quantities, an 'exchange length', $l_{ex} = \sqrt{A/M_s^2}$ and a domain wall thickness $l_w = \sqrt{A/2K}$.

In nanostructured systems however, such as nanoparticles and thin films, the free energy can no longer be parameterised by three such constants. A , M_s and K all vary profoundly with composition, dimensionality and shape. The relativistic effect, spin-orbit coupling, is particularly influential.

For low temperatures, calculations of the characteristics of the free energy (ground state energy) of a magnetic material are all based on an electronic band structure which has a fixed spin-polarisation e.g. a uniform spin-polarisation for a ferromagnet and fixed sublattice spin polarisations for an antiferromagnet. With increasing temperature, spin fluctuations are induced which eventually destroy the long-range magnetic order and hence the overall spin polarization of the system's electronic structure. These collective electron modes interact as the temperature is raised and are dependent upon and affect the underlying electronic structure. For many materials the magnetic excitations can be modelled by associating local spin-polarisation axes with all lattice sites and the orientations vary very slowly on the time-scale of the electronic motions. [7] These 'local moment' degrees of freedom produce local magnetic fields on the lattice sites which affect the electronic motions and are self-consistently maintained by them. By taking appropriate ensemble averages over the orientational configurations the system's magnetic properties can be determined. In this article we review our recent work on incorporating relativistic effects into the 'disordered local moment' (DLM) DFT-based theory which is used in this context to describe the onset and type of magnetic order in many magnetic systems [8,9]. In particular inclusion of relativistic effects into DLM theory produces an ab-initio description of the temperature dependence of magnetic anisotropy of metallic ferromagnets which agrees well with experimental results and deviates qualitatively from simple, widely used models [2,3].

It is well-known that a description of magnetic anisotropy, K , can be provided once relativistic effects such as the spin-orbit coupling on the electronic structure of materials are considered. Over recent years 'first-principles' R-DFT work has been quite successful in describing trends in K for a range of magnetic materials in bulk, film and nanostructured form [5,10,11] at $T = 0\text{K}$, e.g. [12–17]. As well as pinning down the K constants of micromagnetic models which describe phenomena such as magnetisation reversal processes in magnetic recording materials [18], a careful treatment of spin-orbit coupling also has implications for electronic transport effects such as anisotropic magnetoresistance (AMR) [19]. Until only very recently [2,3], however, little attention was paid to how these relativistic consequences might be influenced by the thermally excited 'local moment' fluctuations. Instead the temperature dependence of K and associated quantities are related without justification to single ion anisotropy models developed by Callen and Callen and others over 40 years ago [20]. In this article we review our ab-initio theory for the temperature dependence of magnetic anisotropy which challenges this simple outlook.

This consideration is rather topical. In the search for magnetic data storage media with densities well in excess of $\text{TBytes}/\text{in}^2$, assemblies of increasingly smaller magnetic nanoparticles are being fabricated. [21,22] Thermally driven demagnetisation and loss of data over a reasonable storage period threatens, however, if a particle size limit is breached. A way of fending off this limit is to use materials with high magnetocrystalline anisotropy, K , since the superparamagnetic diameter of a magnetic particle is proportional to $(k_B T/K)^{\frac{1}{3}}$, where $k_B T$ is the thermal energy. [6] Writing to media of very high K material can be achieved by temporary heating. [23,24] K is reduced significantly during the magnetic write process and the information is locked in as the material

cools. Modelling this process and improving the design of high density magnetic recording media therefore requires an understanding of how K varies with temperature. This consideration also affects estimates of the related blocking temperatures of nanoparticles [25].

In the next section we describe and illustrate briefly our magnetic torque-based method for carrying out ab-initio studies of the magnetic anisotropy of nanoparticles, films, multilayers and bulk materials restricted to 0K. This is rather precise and versatile. We then review the well-tried and tested fluctuating local moment picture of magnetism at finite temperatures and go on to show how relativistic effects can be incorporated into it. The next section has results of an application of this theory to the important magnetic material *FePt* where we demonstrate the profound effect of geometrical structure upon magnetic anisotropy. The final section mentions some ongoing and future developments.

2 Ab-initio theory of magnetic anisotropy via the magnetic torque

Magnetocrystalline anisotropy (MAE) is caused largely by spin-orbit coupling and receives an ab-initio description from the relativistic generalisation of spin density functional (R-DFT) theory. [5] Spin-orbit coupling effects are either treated perturbatively or with a fully relativistic theory [12,26]. Typically the total energy, or the single-electron contribution to it (if the force theorem is used), is calculated for two or more magnetisation directions, \hat{n}_1 and \hat{n}_2 separately, and then the MAE is obtained from the difference, ΔF . ΔF is typically small ranging from meV to μeV and high precision in calculating the energies is required. For example, we used this rationale with a fully relativistic theory to study the MAE of magnetically soft, compositionally disordered binary and ternary component alloys [26,27] and the effect upon it of short-range [12] and long range chemical order [28] in harder magnets such as *CoPt* and *FePt*.

Experimentally, measurements of magnetocrystalline anisotropy constants of magnets can be obtained from torque magnetometry [6]. From similar considerations of magnetic torque, ab-initio calculations of MAE can be also made. There are obvious advantages in that a single calculation only is needed and reliance is not placed on the accurate extraction of a small difference between two energies. In particular the torque method has been used to good effect by Freeman and co-workers [29] in conjunction with their state-tracking method to study the MAE of a range of uniaxial magnets including layered systems. Recently we described how to calculate the torque directly and obtain the MAE using spin-polarised, relativistic multiple scattering theory [3]. This scattering theoretical basis makes the approach very versatile and precise, relevant to the study of nanoclusters and thin films [1,4,30] as well as bulk systems [3]. We describe the method briefly here and illustrate it with a calculation of Fe clusters on Pt substrates before proceeding to the finite temperature extension. Full details can be found in ref. [3].

If the free energy of a material magnetised along a direction specified by

$$\hat{n} = (\sin \vartheta \cos \varphi, \sin \vartheta \sin \varphi, \cos \vartheta) \quad (2)$$

is $F^{(\hat{n})}$, then the torque is

$$\vec{T}^{(\hat{n})} = -\frac{\partial F^{(\hat{n})}}{\partial \hat{n}}. \quad (3)$$

The contribution to the torque from the anisotropic part of $F^{(\hat{n})}$ leads to a direct link between the gap in the spin wave spectrum and the MAE by the solution of the equation [31]

$$\frac{d\hat{n}}{dt} = \gamma(\hat{n} \wedge \vec{T}^{(\hat{n})}). \quad (4)$$

where γ is the gyromagnetic ratio. Closely related to $\vec{T}^{(\hat{n})}$ is the variation of $F^{(\hat{n})}$ with respect to ϑ and φ , i.e. $T_\vartheta(\vartheta, \varphi) = -\frac{\partial F^{(\hat{n})}}{\partial \vartheta}$ and $T_\varphi(\vartheta, \varphi) = -\frac{\partial F^{(\hat{n})}}{\partial \varphi}$. As shown by Wang et al. [29], for most uniaxial magnets, which are well approximated by a free energy of the form

$$F^{(\hat{n})} = F_{iso} + K_2 \sin^2 \vartheta + K_4 \sin^4 \vartheta, \quad (5)$$

(where K_2 and K_4 and magnetocrystalline anisotropy constants and F_{iso} is the isotropic part of the free energy), $T_\vartheta(\vartheta = \pi/4, \varphi = 0) = -(K_2 + K_4)$. This is equal to the MAE, $\Delta F = F^{(1,0,0)} - F^{(0,0,1)}$. For a magnet with cubic symmetry so that

$$F^{(\hat{n})} \approx F_{iso} + K_1(\sin^4 \vartheta \sin^2 2\varphi + \sin^2 2\vartheta), \quad (6)$$

a calculation of $T_\varphi(\vartheta = \pi/2, \varphi = \pi/8)$ gives $-K_1/2$, the leading MAE constant.

The derivation of our formalism for \vec{T} starts from the single electron energy sum part of the free energy from R-DFT. In terms of the integrated electronic density of states, $N^{(\hat{n})}(\varepsilon)$, for a system magnetised along a direction (\hat{n}) , this is

$$F^{(\hat{n})} = - \int^{\varepsilon_F^{(\hat{n})}} d\varepsilon N^{(\hat{n})}(\varepsilon). \quad (7)$$

In multiple scattering theory the integrated density of states is written particularly succinctly using the Lloyd formula [32]

$$N^{(\hat{n})}(\varepsilon) = N_0(\varepsilon) - \frac{1}{\pi} \text{Im} \ln \det \left(\underline{\underline{t}}(\hat{n}; \varepsilon)^{-1} - \underline{\underline{G}}_0(\varepsilon) \right), \quad (8)$$

where $\underline{\underline{t}}(\hat{n}; \varepsilon)$ describes an array of single site scattering t-matrices (combined into a super matrix in site and angular momentum space) and $\underline{\underline{G}}_0(\varepsilon)$ specifies the structure constants which contain all the information as to where the scatterers are spatially located. At this point we restrict the discussion to all scatterers being determined by spin-only magnetic fields aligned with a single direction \hat{n} .

At a site i the t-matrix describing the scattering from a scalar potential and vector magnetic field, located in the unit cell surrounding the site, is obtained from the solution of the Dirac equation. Following a Gordon decomposition of the 4-current and neglect of diamagnetic effects, the magnetic field $B(\mathbf{r})\hat{n}$ couples only to the spin-only current. This means that fields $V(\mathbf{r})\tilde{\mathbf{I}}$ and $\tilde{\beta}\tilde{\sigma}_z B(\mathbf{r})$ are included in the Dirac equation [33] where the z-axis of the local coordinate frame is aligned with \hat{n} . ($\tilde{\mathbf{I}}$, $\tilde{\beta}$ and $\tilde{\sigma}$ are the usual 4×4 matrices). A simple transformation produces a t-matrix for the general coordinate frame,

$$t_i(\hat{n}; \varepsilon) = \underline{\underline{R}}(\hat{n}) t_i(\hat{z}; \varepsilon) \underline{\underline{R}}(\hat{n})^+ \quad (9)$$

where $\underline{\underline{R}}(\hat{n}) = \exp i\alpha_{\hat{m}}(\hat{m} \cdot \vec{J})$ where $\alpha_{\hat{m}}$ is the angle of rotation about an axis $\hat{m} = (\hat{z} \wedge \hat{n})/|\hat{z} \wedge \hat{n}|$ and \vec{J} is the total angular momentum. The torque quantity $T_{\alpha_{\hat{a}}}^{(\hat{n})} = -\frac{\partial F^{(\hat{n})}}{\partial \alpha_{\hat{a}}}$, describing the

variation of the total energy with respect to a rotation of the magnetisation about a general axis \hat{u} , is

$$T_{\alpha_{\hat{u}}}^{(\hat{n})} = -\frac{1}{\pi} \int^{\varepsilon_F^{(\hat{n})}} d\varepsilon \operatorname{Im} \frac{\partial}{\partial \alpha_{\hat{u}}} \left[\ln \det \left(\underline{t}(\hat{n}; \varepsilon)^{-1} - \underline{\underline{G}}_0(\varepsilon) \right) \right] \quad (10)$$

which can be written

$$T_{\alpha_{\hat{u}}}^{(\hat{n})} = -\frac{1}{\pi} \int^{\varepsilon_F^{(\hat{n})}} d\varepsilon \operatorname{Im} \sum_i \operatorname{tr} \left(\underline{\tau}_{ii}^{(\hat{n})}(\varepsilon) \frac{\partial}{\partial \alpha_{\hat{u}}} \left(\underline{R}(\hat{n}) \underline{t}(\hat{n}; \varepsilon)^{-1} \underline{R}(\hat{n})^+ \right) \right) \quad (11)$$

where the KKR scattering path operator [34] is

$$\underline{\tau}^{(\hat{n})} = \left(\left(\underline{t}^{(\hat{n})} \right)^{-1} - \underline{\underline{G}}_0 \right)^{-1}. \quad (12)$$

Since $\frac{\partial \underline{R}(\hat{n})}{\partial \alpha_{\hat{u}}} = i(\underline{\vec{J}} \cdot \hat{u}) \underline{R}(\hat{n})$ and $\frac{\partial \underline{R}(\hat{n})^+}{\partial \alpha_{\hat{u}}} = -i(\underline{\vec{J}} \cdot \hat{u}) \underline{R}(\hat{n})^+$, we obtain the key expression

$$T_{\alpha_{\hat{u}}}^{(\hat{n})} = \frac{1}{\pi} \int^{\varepsilon_F^{(\hat{n})}} d\varepsilon \operatorname{Im} i \sum_i \operatorname{tr} \left(\underline{\tau}_{ii}^{(\hat{n})}(\varepsilon) \left[(\underline{\vec{J}} \cdot \hat{u}) \underline{t}(\hat{n}; \varepsilon)^{-1} - \underline{t}(\hat{n}; \varepsilon)^{-1} (\underline{\vec{J}} \cdot \hat{u}) \right] \right). \quad (13)$$

For $T_{\vartheta(\varphi)}^{(\hat{n})}$, $(\underline{\vec{J}} \cdot \hat{u})$ is just $\underline{J}_{y(z)}$.

As an illustration of this approach we show in Figure 1 results of an investigation of the magnetic anisotropy of iron dimers and trimers on an Pt surface [1]. It is evident that the torque T_{ϑ} and hence the MAE drop significantly when going from the dimer to the trimer. Adding the Pt decoration to the three atom cluster, however, restores a high MAE. With the inner F_{e_3} part of the $F_{e_3}Pt_3$ cluster surrounded the variation of the MAE with φ is strongly reduced.

The magnetic anisotropy of a system diminishes rapidly as the temperature is raised from 0K and the rapidity of this decrease is, like magnetic anisotropy itself, strongly affected by the system's geometrical structure - typically the higher the symmetry the faster the collapse. In the next section we show how this effect emerges from a simple 'spin' model and then, later on, from a fully ab-initio interacting electron description of a magnetic material. We will see, however, how the latter is sometimes qualitatively different from the former.

3 Magnetic anisotropy of a single ion model

For a crystal of a magnet the symmetry connection can be made explicit by writing its magnetic anisotropy as $K = \sum_{\gamma} K_{\gamma} g_{\gamma}(\hat{n})$ where the K_{γ} 's are coefficients, \hat{n} is the magnetisation direction and g_{γ} 's are polynomials (spherical harmonics) of the angles ϑ , φ . The g_{γ} 's belong to the fully symmetric representation of the crystal point group - particular examples for uniaxial and cubic magnets have already been used in the last section. As the temperature rises, K decreases rapidly. The key features of the results of the theoretical work carried out over 40 years ago on this effect [20] come from simple classical spin models of magnetic insulators. Here magnetic moments are associated with the lattice sites of the material. The anisotropic behaviour of such a set of localised 'spins' is given by a term in the hamiltonian $H_{an} = \sum_i \sum_{\gamma} k_{\gamma} g_{\gamma}(\hat{e}_i)$ with \hat{e}_i a unit vector denoting the spin direction on the site i . As the temperature is raised, the 'spins' sample the energy surface over a small angular range about the magnetisation direction \hat{n} and

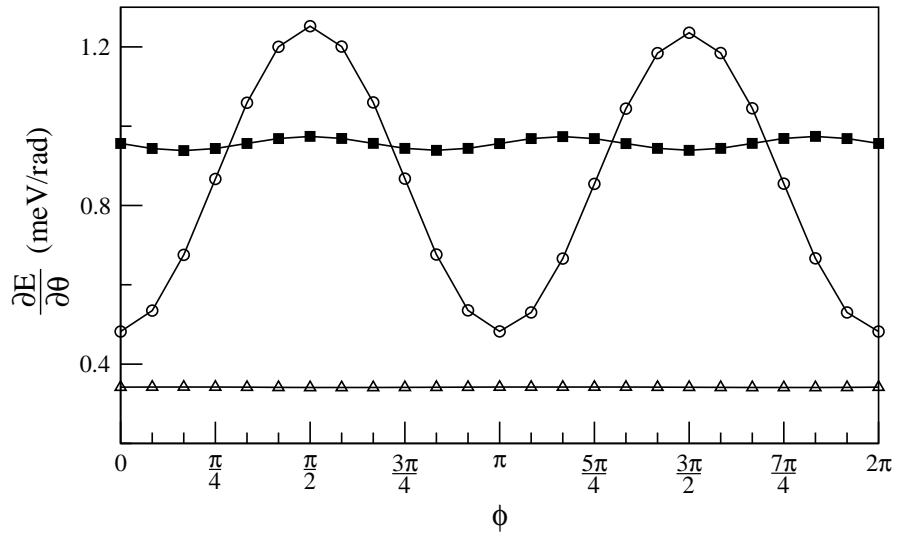
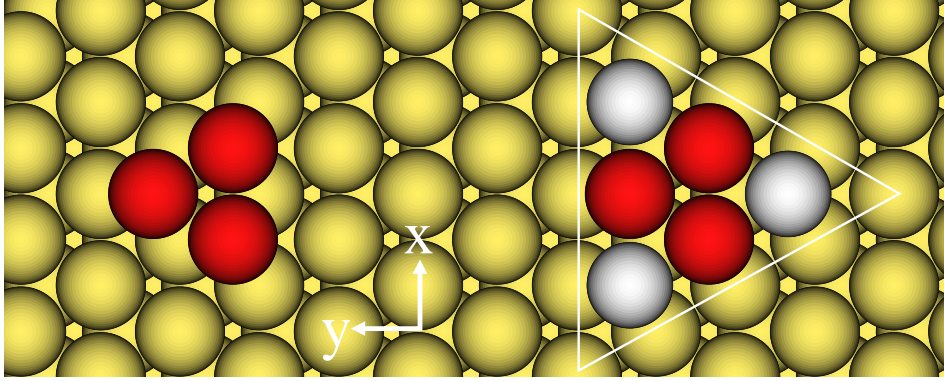


Figure 1: From ref. [1]. Top panel: Structure of a Fe trimer on Pt(111) without (left) and with (right) decoration by three Pt atoms. Bottom panel: torque component $T_\theta(\theta, \phi)$ for Fe₂ (circles), Fe₃ (triangles) and Pt₃Fe₃ (squares) for $\theta = \frac{\pi}{4}$ as a function of the azimuth angle ϕ .

the anisotropy energy is given from the difference between averages taken for the magnetisation along the easy and hard directions. If the coefficients k_γ are assumed to be rather insensitive to temperature, the dominant thermal variation of K for a ferromagnet is given by $K(T)/K(0) = \langle g_l(\hat{e}) \rangle_T / \langle g_l(\hat{e}) \rangle_0$. The averages $\langle \dots \rangle_T$ are taken such that $\langle \hat{e} \rangle_T = m(T)$, the magnetisation of the system at temperature T , and l is the order of the spherical harmonic describing the angular dependence of the local anisotropy i.e. $l = 2$ for a uniaxial system and 4 for a cubic one. At low temperatures $K(T)/K(0) \approx (m(T)/m(0))^{l(l+1)/2}$ and near the Curie temperature T_c , $K(T)/K(0) \approx (m(T)/m(0))^l$.

It is helpful for later discussion of the ab-initio theory to show where these results come from in a little more detail. Consider a classical spin hamiltonian for, say, a uniaxial ferromagnet.

$$H = -\frac{1}{2} \sum_{i,j} J_{ij} \hat{e}_i \cdot \hat{e}_j - k \sum_i (\hat{n}_0 \cdot \hat{e}_i)^2 \quad (14)$$

where \hat{e}_i describes the orientation of a classical spin at site i and J_{ij} and k are exchange and anisotropy parameters. \hat{n}_0 is a unit vector along the magnetic easy axis. A mean field description of the system is given by reference to a hamiltonian $\sum_i \vec{h} \cdot \hat{e}_i$ where the orientation of Weiss field \vec{h} , i.e. $\vec{h} = h\hat{n}$, determines the direction of the magnetisation of the system and has direction cosines $(\sin \vartheta \cos \varphi, \sin \vartheta \sin \varphi, \cos \vartheta)$. Within this mean field approximation the magnetisation m is $\vec{m}(T) = \int \hat{e} P(\hat{e}) d\hat{e}$ where the probability of a spin being orientated along \hat{e} is $P(\hat{e}) = e^{-\beta h \hat{n} \cdot \hat{e}} / Z_0$ with $Z_0 = \int e^{-\beta h \hat{n} \cdot \hat{e}} d\hat{e}$. The free energy difference per site between the system magnetised along two directions \hat{n}_1 and \hat{n}_2 is

$$K(T) = -\frac{k}{Z_0} \int ((\hat{n}_0 \cdot \hat{e})^2 e^{-\beta h \hat{n}_1 \cdot \hat{e}} - (\hat{n}_0 \cdot \hat{e})^2 e^{-\beta h \hat{n}_2 \cdot \hat{e}}) d\hat{e} \quad (15)$$

If \hat{n}_1 and \hat{n}_2 are parallel and perpendicular to the magnetic easy axis \hat{n}_0 respectively then

$$K(T) = -\frac{k}{Z_0} \int g_2(\hat{n}_0 \cdot \hat{e}) e^{-\beta h \hat{n}_0 \cdot \hat{e}} d\hat{e} \quad (16)$$

where g_2 is the Legendre polynomial $(3(\hat{n}_0 \cdot \hat{e})^2 - 1)/2$. As a function of the magnetisation $m(T)/m(0)$, $K(T)/K(0)$ varies as specified above, i.e. quadratically near the Curie temperature T_c and cubically at low T . The same dependence can be shown for this simple spin model for the rate of variation of magnetic anisotropy with angle ϑ that the magnetisation makes with the system's easy axis, namely the magnetic torque [6] $T_\vartheta = -\partial K / \partial \vartheta$.

Of course in a real magnetic system with itinerant electrons it is not correct to apportion electrons among the sites at which the material's nuclei are positioned. Instead it is necessary to return to the fundamentals of R-DFT and to see how a tractable finite temperature generalisation can be worked out.

4 Magnetism at finite temperatures - 'Disordered Local Moments'

In principle the extension of electronic density functional theory to finite temperatures was carried out by Mermin [35] soon after the pioneering papers of Hohenberg, Kohn and Sham [36].

The single particle entropy is included and the effective one-electron fields involve Ω_{xc} , the exchange-correlation part of the Gibbs Free Energy functional of particle and magnetisation densities. Formally this can be expressed in terms of spin-dependent pair correlation functions $g_\lambda(\sigma, \sigma'; \mathbf{r}, \mathbf{r}')$, i.e.

$$\Omega_{xc}[n, \mathbf{m}] = \frac{e^2}{2} \int_0^1 d\lambda \int d\mathbf{r} \int d\mathbf{r}' \sum_{\sigma, \sigma'} \frac{n_\sigma(\mathbf{r})n_{\sigma'}(\mathbf{r}')}{|\mathbf{r} - \mathbf{r}'|} g_\lambda(\sigma, \sigma'; \mathbf{r}, \mathbf{r}') \quad (17)$$

where $n_\sigma(\mathbf{r})$ is the spin resolved density.

It would seem logical then simply to make the finite temperature extension of the LDA (or GGA) that is successfully exploited in applications on the ground state of magnetic materials. So, for example, $\Omega_{xc}[n, \mathbf{m}]$ is replaced by $\int d\mathbf{r} n(\mathbf{r}) \Omega_{xc}^0(n(\mathbf{r}))$ where Ω_{xc}^0 is the exchange-correlation part of the Gibbs Free Energy of a homogeneous electron gas. This assumption allows the thermally averaged magnetisation, \bar{M} , along with the spin splitting of the electronic structure to decrease only by the excitation of particle-hole, ‘Stoner’ excitations across the Fermi surface. However, it severely underestimates the effects of the thermally induced spin-wave excitations. The calculated Curie temperatures are often up to an order of magnitude too high, there is no obvious mechanism for moments in the paramagnetic state and the uniform static paramagnetic susceptibility does not follow a Curie-Weiss behaviour as found for many metallic systems.

Evidently, part of the pair correlation function $g_\lambda(\sigma, \sigma'; \mathbf{r}, \mathbf{r}')$ should be related by the fluctuation dissipation theorem to the magnetic susceptibilities harbouring information about spin waves. These spin fluctuations interact as temperature is increased and so $\Omega_{xc}[n, \mathbf{m}]$ should deviate significantly from the local approximation with a consequent impact upon the form of the effective single electron states. Indeed accounts of modern electronic structure theory for magnetic systems [10, 11] have large sections devoted to work which is concerned with the of modelling spin fluctuation effects whilst maintaining the spin-polarised single electron basis.

Most of this work is based on a rather simple, pervasive picture of fluctuating ‘local moments’ which stems from the belief of a time scale separation of the electronic degrees of freedom. An electron travels from site to site on a much faster timescale than that of the spin waves. So the dominant thermal fluctuation of the magnetisation which the straightforward finite temperature extension of spin-polarised band theory misses can be pictured quite simply as orientational fluctuations of ‘local moments’. These entities are the magnetisations within each unit cell of the underlying crystal lattice which are set up by the collective behaviour of all the electrons. Their orientations persist on timescales long compared to electronic ‘hopping’ times. At low temperatures, their long wavelength, slow spin wave dynamics can be directly extracted from the transverse part of the magnetic susceptibility. At higher temperatures the more complex behaviour can be described with a classical treatment. The energy is considered of the many interacting electron system constrained so that its local magnetisations are oriented along prescribed directions, i.e. a ‘local moment’ configuration. Averages over such orientational configurations are subsequently taken to determine the equilibrium properties of the system. \bar{M} can now vanish as the disorder of the ‘local moments’ grows. There remains, however, the issue as to which fluctuations are the most important.

Formally R-DFT [5, 8] specifies the ‘generalised’ grand potential, $\Omega^{(\hat{n})}(\{\hat{e}\})$, of an itinerant electron system which is constrained in such a way that the site by site spin polarisation axes

are configured according to $\{\hat{e}\} = \{\hat{e}_1, \hat{e}_2, \dots, \hat{e}_N\}$ where N is the number of sites (moments) in the system. The $\{\hat{e}\}$, classical unit vectors, are thus the degrees of freedom describing the local moment orientations and $\Omega^{(\hat{n})}(\{\hat{e}\})$ is the ‘local moment’ hamiltonian. With relativistic effects such as spin-orbit coupling included, magnetic anisotropy can be described. This means that orientations of the local moments with respect to a specified direction \hat{n} within the material are relevant.

One way forward from this point is to carry out calculations of $\Omega^{(\hat{n})}(\{\hat{e}\})$ for a selection of configurations (‘spin’ spirals, 2 impurities in a ferromagnet, magnetically ordered supercells etc.) by making some assumptions about the most dominant fluctuations. One then fits the set of $\Omega^{(\hat{n})}(\{\hat{e}\})$ ’s to a simple functional form. For the non-relativistic limit typically a classical Heisenberg model, $\Omega^{(\hat{n})}(\{\hat{e}\}) = -\frac{1}{2} \sum_{ij} J_{ij} \hat{e}_i \cdot \hat{e}_j$ is set up and various statistical mechanics methods (e.g. Monte Carlo) are used to produce the desired thermodynamic averages. Many useful studies have been carried out in this way but there is a risk that a bias is produced so that some of the physics is missed. The spin polarised electronic structures of the restricted set of constrained systems are not guaranteed to generate magnetic correlations that are consistent with the chosen sampling of the orientational configurations. In other words the electronic and magnetic structures are not necessarily mutually consistent. When spin-orbit coupling effects are included these worries grow - there is the question about what form the anisotropy of the effective spin model should take. Should it, perhaps, be a classical isotropic Heisenberg model with a single site anisotropy term that was illustrated in the last section or will this be inconsistent with the underlying electronic behaviour? In the following we summarise the main points of our ‘disordered local moment’ (DLM) theory which avoids these problems. Full details can be found in references [8,9] and in references [2,3] for the relativistic extension. In particular its description of the temperature dependent magnetic anisotropy can be qualitatively different from that of simple spin models as we will show later.

The ‘disordered local moment’ (DLM) picture is implemented within a multiple-scattering (Korringa-Kohn-Rostoker, KKR) [37–39] formalism. Some applications include the description of the experimentally observed local exchange splitting and magnetic short-range order in both ultra-thin Fe films [40] and bulk Fe [8], the damped RKKY-like magnetic interactions in the compositionally disordered CuMn ‘spin-glass’ alloys [41] and the onset of magnetic order in a range of alloys [42,43]. By combining it with the local self-interaction correction (L-SIC) [44] for strong electron correlation effects, we have also recently used it to account quantitatively for the magnetic ordering in the heavy rare earths [45].

5 Relativistic Disordered Local Moment (R-DLM) Theory

We consider a collinear magnetic system magnetised with reference to a single direction \hat{n} at a temperature T . (A non-collinear generalisation can be made by making the notation more complicated.) The orientational probability distribution is denoted by $P^{(\hat{n})}(\{\hat{e}\})$, and its average

$$\langle \hat{e}_i \rangle = \int \dots \int \hat{e}_i P^{(\hat{n})}(\{\hat{e}\}) d\hat{e}_1 \dots d\hat{e}_N = \hat{n}. \quad (18)$$

is aligned with the magnetisation direction \hat{n} . The canonical partition function and the probability function are defined as

$$Z^{(\hat{n})} = \int \dots \int e^{-\beta \Omega^{(\hat{n})}(\{\hat{e}\})} d\hat{e}_1 \dots d\hat{e}_N, \quad (19)$$

and

$$P^{(\hat{n})}(\{\hat{e}\}) = \frac{e^{-\beta \Omega^{(\hat{n})}(\{\hat{e}\})}}{Z^{(\hat{n})}}, \quad (20)$$

respectively. The thermodynamic free-energy which includes the entropy associated with the orientational fluctuations as well as creation of electron-hole pairs, is given by

$$F^{(\hat{n})} = -\frac{1}{\beta} \ln Z^{(\hat{n})}. \quad (21)$$

By choosing a trial Hamiltonian function, $\Omega_0^{(\hat{n})}(\{\hat{e}\})$ with $Z_0^{(\hat{n})} = \int \dots \int e^{-\beta \Omega_0^{(\hat{n})}(\{\hat{e}\})} d\hat{e}_1 \dots d\hat{e}_N$,

$$P_0^{(\hat{n})}(\{\hat{e}\}) = \frac{e^{-\beta \Omega_0^{(\hat{n})}(\{\hat{e}\})}}{Z_0^{(\hat{n})}} \quad (22)$$

and $F_0^{(\hat{n})} = -\frac{1}{\beta} \ln Z_0^{(\hat{n})}$ the *Feynman-Peierls Inequality* [46] implies an upper bound for the free energy, i.e.,

$$F^{(\hat{n})} \leq F_0^{(\hat{n})} + \left\langle \Omega^{(\hat{n})} - \Omega_0^{(\hat{n})} \right\rangle^0, \quad (23)$$

where the average refers to the probability $P_0^{(\hat{n})}(\{\hat{e}\})$. By expanding $\Omega_0^{(\hat{n})}(\{\hat{e}\})$ as

$$\Omega_0^{(\hat{n})}(\{\hat{e}\}) = \sum_i \omega_i^{1(\hat{n})}(\hat{e}_i) + \frac{1}{2} \sum_{i \neq j} \omega_{i,j}^{2(\hat{n})}(\hat{e}_i, \hat{e}_j) + \dots, \quad (24)$$

the ‘best’ trial system is found to satisfy [8, 9]

$$\left\langle \Omega^{(\hat{n})} \right\rangle_{\hat{e}_i}^0 - \left\langle \Omega^{(\hat{n})} \right\rangle^0 = \left\langle \Omega_0^{(\hat{n})} \right\rangle_{\hat{e}_i}^0 - \left\langle \Omega_0^{(\hat{n})} \right\rangle^0, \quad (25)$$

$$\left\langle \Omega^{(\hat{n})} \right\rangle_{\hat{e}_i, \hat{e}_j}^0 - \left\langle \Omega^{(\hat{n})} \right\rangle^0 = \left\langle \Omega_0^{(\hat{n})} \right\rangle_{\hat{e}_i, \hat{e}_j}^0 - \left\langle \Omega_0^{(\hat{n})} \right\rangle^0, \quad (26)$$

and so on, where $\langle \cdot \rangle_{\hat{e}_i}$ or $\langle \cdot \rangle_{\hat{e}_i, \hat{e}_j}$ denote restricted statistical averages with \hat{e}_i or both \hat{e}_i and \hat{e}_j kept fixed, respectively. (In the following we shall omit the superscript 0 from the averages.)

If we set $\Omega_0^{(\hat{n})}(\{\hat{e}\})$ as a sum of mean field Weiss terms

$$\Omega_0^{(\hat{n})}(\{\hat{e}\}) = \sum_i \vec{h}_i^{(\hat{n})} \cdot \hat{e}_i \quad (27)$$

where $\vec{h}_i^{(\hat{n})} = h_i^{(\hat{n})} \hat{n}$ with

$$h_i^{(\hat{n})} = \int \frac{3}{4\pi} (\hat{e}_i \cdot \hat{n}) \left\langle \Omega^{(\hat{n})} \right\rangle_{\hat{e}_i} d\hat{e}_i. \quad (28)$$

the probability distribution is

$$P_i^{(\hat{n})}(\hat{e}_i) = \frac{\exp\left(-\beta \vec{h}_i^{(\hat{n})} \cdot \hat{e}_i\right)}{Z_i^{(\hat{n})}} = \frac{\beta h_i^{(\hat{n})}}{4\pi \sinh \beta h_i^{(\hat{n})}} \exp\left(-\beta \vec{h}_i^{(\hat{n})} \cdot \hat{e}_i\right). \quad (29)$$

and the average alignment of the local moments, proportional to the magnetisation, is

$$\vec{m}_i^{(\hat{n})} = \int \hat{e}_i P_i^{(\hat{n})}(\hat{e}_i) d\hat{e}_i = m_i^{(\hat{n})} \hat{n} \quad (30)$$

and

$$m_i^{(\hat{n})} = -\frac{d \ln Z_i^{(\hat{n})}}{d(\beta h_i^{(\hat{n})})} = \frac{1}{\beta h_i^{(\hat{n})}} - \coth \beta h_i^{(\hat{n})} = L(-\beta h_i^{(\hat{n})}) \quad (31)$$

follows, where $L(x)$ is the Langevin function. Moreover the free energy of the system is

$$F^{(\hat{n})} = \langle \Omega^{(\hat{n})} \rangle + \frac{1}{\beta} \sum_i \int P_i^{(\hat{n})}(\hat{e}_i) \ln P_i^{(\hat{n})}(\hat{e}_i) d\hat{e}_i. \quad (32)$$

This is the key expression for the evaluation of the magnetic anisotropy energy.

Another way of writing the Weiss field is [8]

$$h_i^{(\hat{n})} = S_i^{1,(\hat{n})} = \frac{\partial \langle \Omega^{(\hat{n})} \rangle}{\partial m_i^{(\hat{n})}} \quad (33)$$

Using equations (29) and (31), this is shown to be equivalent to solving the equation of state

$$\frac{\partial F^{(\hat{n})}}{\partial m_i^{(\hat{n})}} = 0. \quad (34)$$

Note that an identical Weiss field $\vec{h}^{(\hat{n})}$ associated with every site corresponds to a description of a ferromagnetic system magnetised along \hat{n} with no reference to an external field.

The paramagnetic state is given by the Weiss fields being zero so that the probabilities, $P_i^{(\hat{n})} = \frac{1}{4\pi}$ and on any site a moment has an equal chance of pointing in any direction. This means the magnetisations, $m_i^{(\hat{n})}$ vanish. The magnetic transition temperature, onset and type of magnetic order can be extracted by studying the effects of a small inhomogeneous magnetic field on this high T paramagnetic state [8, 9]. From the equation of state when the effects of the external magnetic field are included the paramagnetic susceptibility can be obtained [8]

$$\chi_{ij} = \frac{\beta}{3} \sum_k S_{ik}^{2,(\hat{n})} \chi_{kj} + \frac{\beta}{3} \delta_{ij} \quad (35)$$

where

$$S_{ik}^{2,(\hat{n})} = \frac{\delta^2 \langle \Omega^{(\hat{n})} \rangle}{\delta m_i^{(\hat{n})} \delta m_k^{(\hat{n})}} = \frac{9}{16\pi^2} \int \int (\hat{e}_i \cdot \hat{n}) \langle \Omega^{(\hat{n})} \rangle_{\hat{e}_i, \hat{e}'_k} (\hat{e}'_k \cdot \hat{n}) d\hat{e}_i d\hat{e}'_k \quad (36)$$

5.1 The role of the CPA

In our work we carry out the averaging over local moment configurations using Coherent Potential Approximation (CPA) [38, 39, 47] technology. The electronic charge density and also the magnetisation density, which sets the magnitudes, $\{\mu\}$, of the local moments, are determined from a self-consistent field (SCF)-KKR-CPA [39] calculation. For a given set of (self-consistent) potentials, electronic charge and local moment magnitudes the orientations of the local moments are accounted for by the similarity transformation of the single-site t-matrices [48],

$$\underline{t}_i(\hat{e}_i) = \underline{R}(\hat{e}_i) \underline{t}_i(\hat{z}) \underline{R}(\hat{e}_i)^+ , \quad (37)$$

where for a given energy (not labelled explicitly) $\underline{t}_i(\hat{z})$ stands for the t -matrix with effective field pointing along the local z axis [33] and $\underline{R}(\hat{e}_i)$, as before, is a unitary representation of the $O(3)$ transformation that rotates the z axis along \hat{e}_i .

The CPA determines an effective medium through which the motion of an electron mimics the motion of an electron *on the average*. In a system magnetised along a direction \hat{n} , the medium is specified by t -matrices, $\underline{t}_{i,c}^{(\hat{n})}$, which satisfy the condition [38],

$$\langle \underline{\mathcal{T}}_{ii}^{(\hat{n})}(\{\hat{e}\}) \rangle = \int \langle \underline{\mathcal{T}}_{ii}^{(\hat{n})} \rangle_{\hat{e}_i} P_i^{(\hat{n})}(\hat{e}_i) d\hat{e}_i = \underline{\mathcal{T}}_{ii,c}^{(\hat{n})}, \quad (38)$$

where the site-diagonal matrices of the multiple scattering path operator [34] are defined as,

$$\langle \underline{\mathcal{T}}_{ii}^{(\hat{n})} \rangle_{\hat{e}_i} = \underline{\mathcal{T}}_{ii,c}^{(\hat{n})} \underline{D}_i^{(\hat{n})}(\hat{e}_i), \quad (39)$$

$$\underline{D}_i^{(\hat{n})}(\hat{e}_i) = \left(\underline{1} + \left[\underline{t}_i(\hat{e}_i)^{-1} - \left(\underline{t}_{i,c}^{(\hat{n})} \right)^{-1} \right] \underline{\mathcal{T}}_{ii,c}^{(\hat{n})} \right)^{-1}, \quad (40)$$

and

$$\underline{\mathcal{T}}_c^{(\hat{n})} = \left(\left(\underline{t}_{i,c}^{(\hat{n})} \right)^{-1} - \underline{G}_0 \right)^{-1}. \quad (41)$$

Eq. (38) can be rewritten in terms of the excess scattering matrices,

$$\underline{X}_i^{(\hat{n})}(\hat{e}_i) = \left(\left[\left(\underline{t}_{i,c}^{(\hat{n})} \right)^{-1} - \underline{t}_i(\hat{e}_i)^{-1} \right]^{-1} - \underline{\mathcal{T}}_{ii,c}^{(\hat{n})} \right)^{-1}, \quad (42)$$

in the form

$$\int \underline{X}_i^{(\hat{n})}(\hat{e}_i) P_i^{(\hat{n})}(\hat{e}_i) d\hat{e}_i = \underline{0}. \quad (43)$$

Thus, for a given set of Weiss fields, $h_i^{(\hat{n})}$, and corresponding probabilities, $P_i^{(\hat{n})}(\hat{e}_i)$ Eq.(43) can be solved by iterating together with Eqs.(42) and (41) to obtain the matrices, $\underline{t}_{i,c}^{(\hat{n})}$ [3].

Using the magnetic force theorem again the single-particle energy part of the R-DFT Grand Potential gives

$$\Omega^{(\hat{n})}(\{\hat{e}\}) \simeq - \int d\varepsilon f_{FD}(\varepsilon; \nu^{(\hat{n})}) N^{(\hat{n})}(\varepsilon; \{\hat{e}\}), \quad (44)$$

as an effective ‘local moment’ Hamiltonian. where $\nu^{(\hat{n})}$ is the chemical potential, $f_{FD}(\varepsilon; \nu^{(\hat{n})})$ is the Fermi-Dirac distribution, and $N^{(\hat{n})}(\varepsilon; \{\hat{e}\})$ denotes the integrated density of states for the orientational configuration, $\{\hat{e}\}$. From the Lloyd formula [32] $N^{(\hat{n})}(\varepsilon; \{\hat{e}\})$,

$$N^{(\hat{n})}(\varepsilon; \{\hat{e}\}) = N_0(\varepsilon) - \frac{1}{\pi} \text{Im} \ln \det \left(\underline{t}^{(\hat{n})}(\varepsilon; \{\hat{e}\})^{-1} - \underline{G}_0(\varepsilon) \right), \quad (45)$$

($N_0(\varepsilon)$ being the integrated DOS of the free particles) and properties of the CPA effective medium, the partially averaged electronic Grand Potential is given by

$$\begin{aligned} \langle \Omega^{(\hat{n})} \rangle_{\hat{e}_i} &= - \int d\varepsilon f_{FD}(\varepsilon; \nu^{(\hat{n})}) N_c^{(\hat{n})}(\varepsilon) + \frac{1}{\pi} \int d\varepsilon f_{FD}(\varepsilon; \nu^{(\hat{n})}) \text{Im} \ln \det \underline{M}_i^{(\hat{n})}(\varepsilon; \hat{e}_i), \\ &+ \sum_{j \neq i} \frac{1}{\pi} \int d\varepsilon f_{FD}(\varepsilon; \nu^{(\hat{n})}) \text{Im} \langle \ln \det \underline{M}_j^{(\hat{n})}(\varepsilon; \hat{e}_j) \rangle, \end{aligned} \quad (46)$$

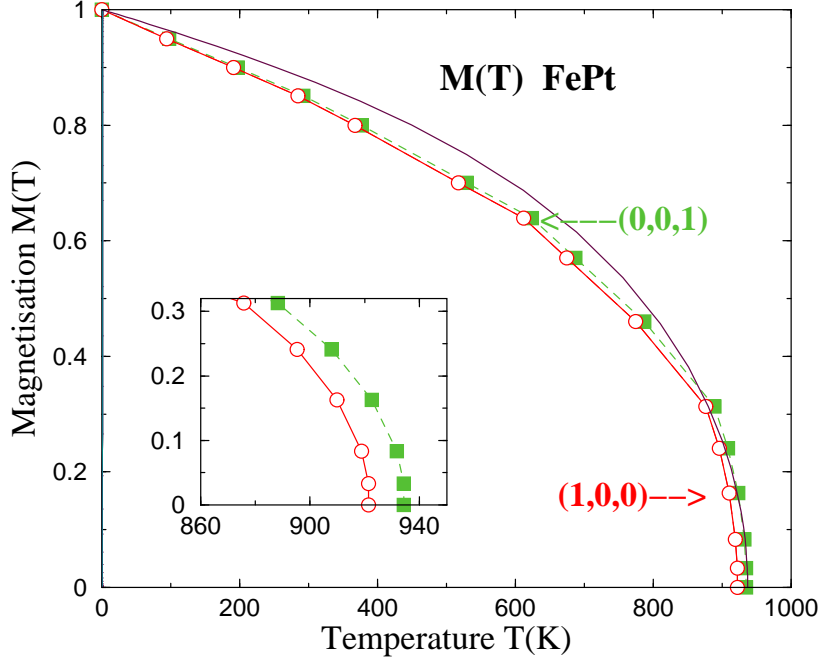


Figure 2: The magnetisation of FePt versus temperature [2]. The filled squares/open circles refer to a magnetisation along $\hat{n} = (0, 0, 1)/(1, 0, 0)$. In the inset, near T_c , the lower intercept shows what T_c would be with the system constrained to become magnetically ordered along $(1, 0, 0)$.

and the Weiss field, $h_i^{(\hat{n})}$, can be expressed, using Eq.(28), as

$$h_i^{(\hat{n})} = \frac{3}{4\pi} \int (\hat{e}_i \cdot \hat{n}) \left[\int d\varepsilon f_{FD}(\varepsilon; \nu^{(\hat{n})}) \frac{1}{\pi} \text{Im} \ln \det \underline{M}_i^{(\hat{n})}(\varepsilon; \hat{e}_i) \right] d\hat{e}_i. \quad (47)$$

where $\underline{M}_i^{(\hat{n})}(\varepsilon; \hat{e}_i) = \left(\underline{1} + \left[(\underline{t}_i(\hat{e}_i))^{-1} - (\underline{t}_{i,c}^{(\hat{n})})^{-1} \right] \underline{\mathcal{T}}_{ii,c}^{(\hat{n})} \right)$ and $N_c^{(\hat{n})}(\varepsilon) = -\frac{1}{\pi} \text{Im} \ln \det \left(\underline{t}_c^{(\hat{n})}(\varepsilon)^{-1} - \underline{G}_0(\varepsilon) \right)$.

The solution of Eqs.(47) and (31) produces the variation of the magnetisation $m_i^{(\hat{n})}$ with temperature T with $m_i^{(\hat{n})}$ going to zero at $T = T_c^{(\hat{n})}$. When relativistic effects are included, the magnetisation direction \hat{n} for which $T_c^{(\hat{n})}$ is highest indicates the easy direction for the onset of magnetic order. We can define a temperature range $\Delta T_{aniso} = T_c^{(\hat{n}_e)} - T_c^{(\hat{n}_h)}$ where \hat{n}_e and \hat{n}_h are the system's high temperature easy and hard directions respectively, which is related to the magnetic anisotropy of the system at lower temperatures. In Figure 2 we show the example of the hard magnet $L1_0$ -ordered-FePt. T_c is at 935K with the easy axis, $(0, 0, 1)$. This mean field approximation is in reasonable agreement with the experimental value of 750K. (An Onsager cavity field technique could be used to improve this estimate, see [9], without affecting the quality of the following results for the MAE.) The full line shows the mean field approximation to a classical Heisenberg model for comparison.

6 A torque-based formula for the magnetisation dependence of magnetic anisotropy

We return to Eq.(32) for the expression for the free energy $F^{(\hat{n})}$ of a system magnetised along a direction $\hat{n} = (\sin \vartheta \cos \varphi, \sin \vartheta \sin \varphi, \cos \vartheta)$ and consider how it varies with change in magnetisation angles ϑ and φ , i.e. $T_{\vartheta} = -\frac{\partial F^{(\hat{n})}}{\partial \vartheta}$, $T_{\varphi} = -\frac{\partial F^{(\hat{n})}}{\partial \varphi}$. Since the single site entropy term in Eq.(32) is invariant with respect to the angular variations we can write

$$T_{\vartheta(\varphi)} = -\frac{\partial}{\partial \vartheta(\varphi)} \left[\sum_i \int P_i^{(\hat{n})}(\hat{e}_i) \langle \Omega^{(\hat{n})} \rangle_{\hat{e}_i} d\hat{e}_i \right]. \quad (48)$$

By using Eq.(46) together with properties of the CPA effective medium [3], we find directly

$$T_{\vartheta(\varphi)} = -\frac{\text{Im}}{\pi} \int d\varepsilon f_{FD}(\varepsilon; \nu^{(\hat{n})}) \left[\sum_i \int \frac{\partial P_i^{(\hat{n})}(\hat{e}_i)}{\partial \vartheta(\varphi)} \ln \det \underline{M}_i^{(\hat{n})}(\varepsilon; \hat{e}_i) d\hat{e}_i \right] \quad (49)$$

According to the form of $P_i^{(\hat{n})}(\hat{e}_i)$ given in Eq. (29) the principal expression for the magnetic torque at finite temperature is thus

$$T_{\vartheta(\varphi)} = \frac{\text{Im}}{\pi} \int d\varepsilon f_{FD}(\varepsilon; \nu^{(\hat{n})}) \left[\sum_i \int \beta h_i P_i^{(\hat{n})}(\hat{e}_i) \left(\frac{\partial \hat{n}}{\partial \vartheta(\varphi)} \cdot \hat{e}_i \right) \ln \det \underline{M}_i^{(\hat{n})}(\varepsilon; \hat{e}_i) d\hat{e}_i \right]. \quad (50)$$

For a uniaxial ferromagnet such as a $L1_0$ 3d-4d/5d transition metal magnet or a magnetic thin film, the performance of a single CPA calculation for appropriate values of the energy ε is carried out at fixed values of the βh_i products (and therefore a chosen magnetisation m) and for the system magnetised along $\hat{n} = (\sin \pi/4, 0, \cos \pi/4)$. Subsequent evaluation of our torque expression, Eq.(50), i.e. $-T_{\vartheta}(\vartheta = \pi/4, \varphi = 0)$ yields the sum of the first two magnetic anisotropy constants K_2 and K_4 . Similarly $-T_{\varphi}(\vartheta = \pi/2, \varphi = \pi/8)$ gives an estimate of the leading constant $K_1/2$ for a cubic system. It can be shown [3] that the expression we found for $T_{\vartheta(\varphi)}$ for a magnet at $T = 0\text{K}$, Eq.(13), is equivalent to Eq.(49) for the limit $\beta h \rightarrow \infty$, i.e. when $T \rightarrow 0\text{K}$.

7 Ferromagnets with tetragonal and cubic crystal symmetry

We compare the MAE of $FePt$ in both its ordered $L1_0$ phase with tetragonal symmetry and in its compositionally disordered $Fe_{50}Pt_{50}$ cubic phase in figures 3 and 4 respectively.

Figure 3 shows the magnetic anisotropy energy, $\Delta F((0, 0, 1), (1, 0, 0)) = -(K_2 + K_4)$ versus the square of the magnetisation. For all temperatures the magnetic easy axis is perpendicular to the layering in the $L1_0$ ordered structure in line with experiment [49, 50]. The approximate m^2 variation of ΔF is a clear consequence of the itinerant nature of the magnetism in this system. Notably the magnetisation dependence agrees well with experiment [23, 51] and differs significantly from that produced by the single ion model, also shown in the figure. With hindsight, as shown in the figure, we find our the ab-initio results fit quite well to those of classical anisotropic Heisenberg model

$$H = -\frac{1}{2} \sum_{i,j} (J^{\parallel} (e_{x,i} e_{x,j} + e_{y,i} e_{y,j}) + J^{\perp} e_{z,i} e_{z,j}) \quad (51)$$

where $J^{\parallel} - J^{\perp} = -1.835\text{meV}$.

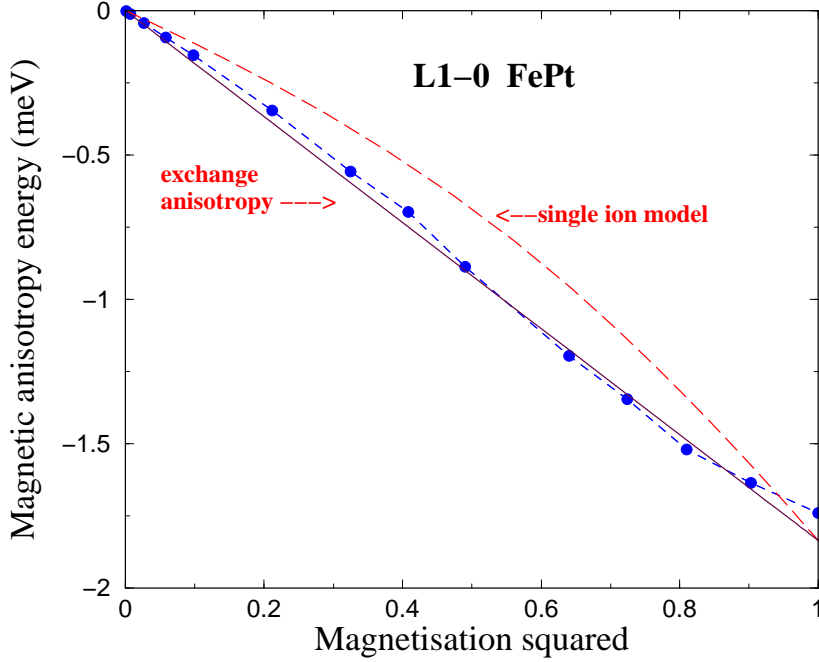


Figure 3: The magnetic anisotropy of $L1_0$ -FePt as a function of the square of magnetisation. The filled circles show the calculations from the ab-initio theory, the full line the pair-wise anisotropic exchange model $K_0(m(T)/m(0))^2$ and the dashed line the single-ion model function $K_0 \langle g_2(\hat{e}) \rangle_T / \langle g_2(\hat{e}) \rangle_0$ with $K_0 = -1.835\text{meV}$.

Mryasov et al. [52] have also described the magnetic anisotropy of $L1_0$ -FePt using a local moment model Hamiltonian with exchange anisotropy, dipolar and single ion anisotropy terms. The parameters were found from with $T = 0\text{K}$ electronic structure calculations.

Crystal structure has a profound effect upon the magnetic anisotropy. Magnetic anisotropy within a single ion anisotropy model decreases according to $m^{l(l+1)/2}$ at low T , ($m \approx 1$) and proportional to m^l for small m at higher T . For materials with tetragonal symmetry, $l = 2$, as shown in Fig.3. On this basis a cubic magnet's MAE should possess an m dependence where $l = 4$, i.e. m^{10} at low T and m^4 at higher T . This single ion pattern is not manifested in our ab-initio results of disordered $Fe_{50}Pt_{50}$ shown in Figure 4 [3]. In this system the lattice sites of the f.c.c. lattice are occupied at random by either Fe or Pt atoms. The cubic symmetry causes this alloy to be magnetically very soft. Indeed the overall scale of the MAE is some three orders of magnitude smaller than its $L1_0$ -ordered counterpart shown in Fig.3. Ordering into a tetragonal $L1_0$ structure of layers of predominantly Fe atoms stacked alternately with Pt layers along the $(1, 0, 0)$ direction causes a significant increase of K . Okamoto et al [51] have measured K of $FePt$ carefully as a function of compositional order and the trend, for $T = 0\text{K}$, has been successfully reproduced in ab-initio calculations [28, 53].

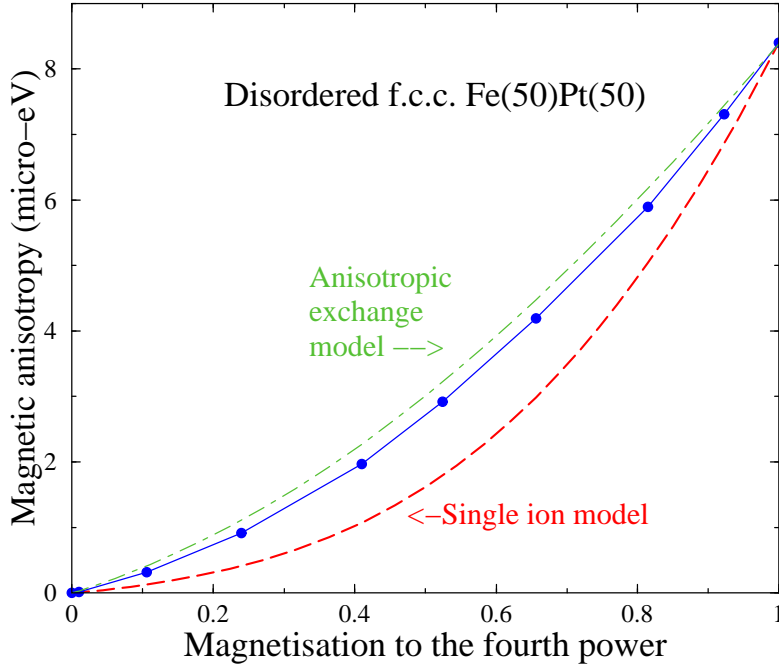


Figure 4: The magnetic anisotropy constant K_1 of the cubic magnet $\text{Fe}_{50}\text{Pt}_{50}$ as a function of the fourth power of the magnetisation, m^4 . The filled circles show the calculations from the ab-initio theory, the dashed line from the single-ion anisotropy model $k \sum_i (e_{x,i}^2 e_{y,i}^2 + e_{y,i}^2 e_{z,i}^2 + e_{z,i}^2 e_{x,i}^2)$ and the dot-dashed line from the anisotropic exchange two ion model $\frac{1}{2} \Delta J \sum_{i,j} (e_{x,i}^2 e_{y,j}^2 + e_{y,i}^2 e_{z,j}^2 + e_{z,i}^2 e_{x,j}^2)$ with $k = \Delta J = 8.4 \mu\text{eV}$.

We find a Curie temperature of disordered f.c.c. $\text{Fe}_{50}\text{Pt}_{50}$ of 1085K, again a mean field value which is in reasonable agreement with the experimental value of 750K [51]. Figure 4 shows our calculations [3] of the magnetisation dependence of the leading magnetic anisotropy constant K_1 (Eq.6). As expected K_1 decreases rapidly with temperature - Fig. 4 depicts K_1 versus the fourth power of the magnetisation. At low T , K_1 varies approximately as m^7 whereas this dependence becomes m^4 for smaller M and higher T . Fig.4 also shows the behaviour of the single ion model for a cubic system for comparison. As with the uniaxial metallic magnets already investigated, the ab-initio R-DLM results differ significantly. Again with hindsight an interpretation of the ab-initio results can be given by a model which includes both two site anisotropic exchange and single site anisotropy.

It is interesting to note that in some recent work on thin films we have found that thermally induced magnetisation reorientation transitions we calculated for itinerant magnetic thin films can be interpreted as a trade off between single ion and exchange anisotropy aspects [4].

8 Conclusions

In this article we have shown how the account of fluctuating local moments provided by the R-DLM describes well the temperature dependence of magnetic anisotropy. There is work in progress to look at the magnetic structures of thin films and multilayers and also the blocking temperatures of magnetic nanoparticles. Strongly correlated electron effects are also currently

being included via the Local Self-Interaction Correction (L-SIC) method [44] so that gamut of magnetic materials can be investigated. At the heart of the R-DLM theory is the fully relativistic electronic structure which is affected by and sustains the fluctuating moments. As the temperature of a material is increased the fluctuations grow and the electronic structure changes in consequence. This means that a quantitative theory for the T -dependence of spectroscopic measurements is possible. Indeed an early prediction [8] of the DLM theory was the local exchange splitting in b.c.c. Fe observed above T_c . Significantly and of relevance to spintronics the temperature dependence of transport properties can be covered- ‘spin’-disorder scattering can be carefully considered. The evolution of the resistivity of materials which are inferred to be half-metallic at $T = 0K$ are rather pertinent examples. A quantitative theory of anisotropic magnetoresistivity is another promising project.

References

- [1] S.Bornemann *et al.*, European Phys.J. D, (2007), DOI:10.1140/epjd/e2007-00190-9.
- [2] J.B.Staunton *et al.*, Phys. Rev. Lett. **93**, 257204, (2004).
- [3] J.B.Staunton *et al.*, Phys. Rev. B **74**, 144411, (2006).
- [4] A.Buruzs *et al.*, Phys. Rev. B, in press.
- [5] H.J.F.Jansen, Phys. Rev. B **59**, 4699 (1999).
- [6] R.C.O’Handley, *Modern Magnetic Materials*, (Wiley, 2000).
- [7] *Electron Correlations and Magnetism in Narrow Band System*, edited by T. Moriya (Springer, N.Y., 1981).
- [8] B.L.Gyorffy *et al.*, J. Phys. F: Met. Phys. **15**, 1337 (1985); J.B.Staunton *et al.*, J. Phys. F: Met. Phys. **15**, 1387, (1985).
- [9] J.B.Staunton and B.L.Gyorffy, Phys. Rev. Lett. **69**, 371 (1992).
- [10] J.Kubler, *Theory of itinerant electron magnetism*, (Oxford: Clarendon 2000).
- [11] J.B.Staunton, Rep.Prog. Phys. **57**, 1289, (1994).
- [12] S.S.A.Razee *et al.*, Phys. Rev. Lett. **82**, 5369, (1999).
- [13] A.B.Shick *et al.*, Phys. Rev. B **56**, R14259, (1997).
- [14] T.Burkert *et al.*, Phys. Rev. B **69**, 104426, (2004).
- [15] B.Lazarovits *et al.*, J. Phys.: Cond. Matt.**16**, S5833, (2004).
- [16] X.Qian and W.Hubner, Phys. Rev. B **64**, 092402, (2001).
- [17] I.Cabria *et al.*, Phys. Rev. B **63**, 104424, (2001).

- [18] e.g. H.Kronmuller *et al.*, J.Mag.Magn.Mat. **175**, 177, (1997); M.E.Schabes, J.Mag.Magn.Mat. **95**, 249-288, (1991).
- [19] D.V.Baxter *et al.*, Phys.Rev. B **65**, 212407, (2002); K.Hamaya *et al.*, J.Appl.Phys. **94**, 7657-61, (2003); A.B.Shick *et al.*, Phys.Rev. B **73**, 024418, (2006).
- [20] H.B.Callen and E.Callen, J.Phys.Chem.Solids, **27**, 1271, (1966); N.Akulov, Z. Phys. **100**, 197, (1936); C.Zener, Phys. Rev. **B96**, 1335, (1954).
- [21] S.Sun *et al.*, Science **287**, 1989, (2000).
- [22] X.W.Wu *et al.*, Appl. Phys. Lett. **82**, 3475, (2003).
- [23] J.-U.Thiele *et al.*, J. Appl. Phys. **91**, 6595, (2002).
- [24] A.Lyberatos and K.Y.Guslienko, J. Appl. Phys. **94**, 1119, (2003); H.Saga *et al.*, Jpn. J. Appl. Phys. Part 1 **38**, 1839, (1999); M.Alex *et al.*, IEEE Trans. Magn. **37**, 1244, (2001).
- [25] V.Skumryev *et al.*, Nature, **423**, 850, (2003).
- [26] S.S.A.Razee *et al.*, Phys. Rev. **B56**, 8082 (1997).
- [27] S.Ostanin *et al.*, Phys. Rev. **B69**, 064425, (2004).
- [28] S.Ostanin *et al.*, J.Appl.Phys.**93**, 453, (2003); J.B.Staunton *et al.*,J. Phys.: Cond. Matt.**16**, S5623, (2004).
- [29] X.Wang *et al.*, Phys. Rev. B **54**, 61-64, (1996).
- [30] A.Buruzs *et al.*, J.Mag.Magn.Mat., (2007), DOI:10.1016/j.jmmm.2007.03.179.
- [31] A.I. Akhiezer, V.G.Baryakhtar and S.V.Peletminskii, *Spin Waves and Magnetic Excitations*, (Amsterdam: North Holland), (1968).
- [32] P.Lloyd and P.R.Best, J.Phys.C **8**, 3752, (1975).
- [33] P.Strange *et al.*, J.Phys. C **17**, 3355-71, (1984).
- [34] B.L.Gyorffy and M.J.Stott, in *Band Structure Spectroscopy of Metals and Alloys*, eds.: D.J.Fabian and L.M.Watson, (Academic Press, New York), (1973).
- [35] N.D.Mermin, Phys.Rev. **137**, A1441, (1965).
- [36] P.Hohenberg and W.Kohn, Phys.Rev. **136**, B864, (1964); W.Kohn and L.J.Sham, Phys.Rev.**140**, A1133, (1965).
- [37] J.Korringa, Physica **13**, 392, (1947); W.Kohn and N.Rostoker, Phys.Rev. **94**, 1111, (1954).
- [38] G.M.Stocks *et al.*, Phys. Rev. Lett. **41**, 34, (1978).
- [39] G.M.Stocks and H.Winter, Z.Phys.B **46**, 95, (1982); D.D.Johnson *et al.*, Phys. Rev. Lett. **56**, 2088, (1986).
- [40] S.S.A. Razee *et al.*, Phys. Rev. Lett. **88**, 147201, (2002).

- [41] M.F.Ling *et al.*, Europhys.Lett. **25**, 631, (1994).
- [42] J.B.Staunton *et al.*, J. Phys.: Cond. Matt. **9**, 1281-1300, (1997).
- [43] V.Crisan *et al.*, Phys. Rev. B **66**, 014416, (2002).
- [44] M.Lueders *et al.*, Phys. Rev. B **71**, 205109, (2005).
- [45] I.Hughes *et al.*, Nature, **446**, 650, (2007).
- [46] R.P.Feynman, Phys. Rev. **97**, 660, (1955).
- [47] P.Soven, Phys.Rev. **156**, 809, (1967).
- [48] A.Messiah, *Quantum Mechanics*, (Amsterdam: North Holland), (1965).
- [49] O.A.Ivanov *et al.*, Fiz. Met. Metalloved. **35**, 92, (1973).
- [50] R.F.Farrow *et al.*, J. Appl. Phys. **79**, 5967,(1996).
- [51] S.Okamoto *et al.*, Phys. Rev. B**66**, 024413, (2002).
- [52] O.Mryasov *et al.*, Europhys.Lett. **69**, 805, (2005); R.Skomski *et al.*, J. Appl. Phys. **99**, 08E916, (2006).
- [53] T.Burkert *et al.*, Phys. Rev. B **71**, 134411, (2005).